ANTIMICROBIAL EVALUATION OF *Annona muricata* SEED MEDIATED SYNTHESIZED MANGANESE OXIDE NANOPARTICLES

Supported by tetfund

S. A. Mamuru[1,2]*, C. Okoye[2], A. E. Eseyin[2] and M. B. Dalen[2]
[1]Department of Chemistry, Adamawa State University, Mubi, Nigeria
[2]Department of Chemistry, University of Jos, Plateau State, Nigeria
*Corresponding author: almanto1@yahoo.com

Received: July 19, 2020 **Accepted:** October 13, 2020

Abstract: Green synthesis of metal nanoparticles is an interesting and expanding research area due to the potential applications for the eco-friendly development of novel technologies. Present study report a simple, convenient and low cost method for the synthesis of manganese oxide nanoparticles by reducing potassium permanganate with the help of easily available natural product viz *Annona muricata* seed extract. The characterization of the nanoparticle was done using UV-visible, FTIR and XRD spectroscopic techniques. The morphology of the manganese oxide was confirmed by SEM. The antimicrobial activities of synthesized MnO nanoparticles were observed with higher antimicrobial activity than the standard drug against *S.aureus* and exhibited similar inhibition activity to standard drug against *E. coli*.

Keywords: *Annona muricata* seed, antimicrobial activity, manganese oxide nanoparticles

Introduction

Metal nanoparticles have been produced physically and chemically for a long time. However, recently, their biological production has been investigated, results shows that these nanoparticles exhibit some form of similarities as those produced by chemical or physical methods. The nanoparticles produced by this method have gained considerable importance due to the enhancement of their chemical, physical and biological properties.Biological entities such asflavones, proteins, steroids, carbohydrates, polyphenols etc. known as phytochemicals present in plants facilitates the production of the nanoparticles.

Metal oxides nanoparticles have been studied by a lot of researchers in the last few years due to their structural and magnetic properties which have given themthe potential to be applied in various fields such as electronic, optical, and mechanical devices (Ng *et al*., 2013; Singh *et al*., 2018; Chavali and Nikolova, 2019). They also show good antimicrobial properties due to their large surface area to volume ratio which increases their microbial resistance to metal ions and their non-toxic nature when compared to organic disinfectants. Therefore, metal oxide nanoparticles have attracted the attention of researchers for possible use in biomedical and pharmaceutical applications as alternative effective microbial inhibitors.

The plethora of pathogenic microorganisms found in clinical environment that caused wide range of diseases and death,have led to theemergence of next generation of antibiotic drugs or agents to control microbes,which should be an effective and inexpensive therapeutic approach. Metal oxide nanoparticles offer such possibilities.Various metal oxide nanoparticles were investigated in the field of antimicrobial development (Azam *et al*., 2012). As an important functional metal oxide, manganese oxide has attracted the attention of researchers (Chen and He, 2008; Wang *et al.*, 2008; Xiao *et al.*, 2010); however, very limited information is available on the antimicrobial properties of manganese metal oxide nanoparticles (Jayandra *et al*., 2015; Krishnan and Mahalingam, 2017; Ogunyemi *et al*., 2019).

As our contribution to the development of an emerging area in science and technology, we hereby report the synthesis of manganese oxide nanoparticles using *Annona muricata* seed extract as reducing and capping agent and evaluate its antimicrobial activity against *S. aureus*, *E. coli*, *B. subtilis* and *S. bacillus.*

Materials and Method

Collection of seeds

Mature *Annona muricata* was identified and obtained from Michael Okpara University of Agriculture, Umudike, Abia State. The fruits were sorted from a selection of several mature fruits. The fruits maturity was determined by its dark skin with smooth numerous fleshy spines. The fruit was washed and cut vertically into two halves and the seeds were extracted manually and sun dried (Fig. 1). The dried seeds were crushed to very fine particles using mortar and pestle.

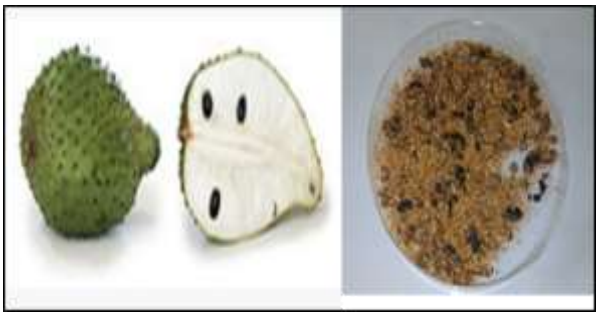

Fig. 1: Fresh fruit and crushed dried seeds of *Annona muricata*

Preparation of Annona muricataseed extract

10 g of the crushed seeds was weighed into a conical flask and 100 ml of deionized water added. The mixture was heated to 100^0C with continuous stirring using a magnetic stirrer for 15 min, then cooled at room temperature and filtered via Whatman filter paper 1 to obtain the fresh extract.

Preparation of potassium permanganate solution

0.01M of potassium permanganate solution was prepared by dissolving potassium permanganate crystals (0.158 g) in 1000 ml volumetric flask and made up to the mark with deionized water.

Preparation of manganese oxide nanoparticles (MnONPs)

An aqueous solution of potassium permanganate (10 mM) was used for the synthesis of MnONPs. Deionised water was used throughout the reaction. pH and temperature were maintained at particular extent to get better result. The manganese ions are reduced by the addition of the freshly prepared *Annona muricata* seed extract (10 ml) in drops to permanganate solution (10 ml) in a beaker with continuous stirring for the proper reduction of the metal ions. The reaction mixture was kept on the magnetic hot stirrer at 50-

60^0C for 2 h until the colour changes from purple to yellowish brown which denoted the metal ion reduction. The mixture was allowed to stand for 24 h during which the solution colour changed from yellowish brown to a permanent reddish brown colour which indicated the complete stabilization of MnONPs. The main factors, pH was maintained between 3 and 4 and the temperature was at 50-60^0C throughout the experiment. The product was then centrifuged at 3500 rpm for 15 min, washed with deionised water and allowed to dry at room temperature to obtain the pure MnO NPs.

Antimicrobial activity

The antimicrobial activity was carried out by agar well diffusion method as described by Gomes *et al*. (2002), against four microbes (*S. aureus*, *E. coli*, *B. subtilis* and *S. bacillus*). Approximately, 105 CFU/ml of inoculums were prepared using Sabouraud's dextrose agar (SDA) by suspending for 6 h. The sample of NPs with antibiotic and solvent blanks (SDA and acetic acid) was filled in the wells of the agar and microbial plates were incubated at 37°C for 72 h. Standard antibiotic, chloramphenicol (concentration 1 mg/ml) was used as positive control. The diameters of zone of inhibition observed were measured and studied.

Results and Discussion

Reaction colour

Figure 2 shows the purple colour aqueous solution of potassium permanganate, milky colour of *Annona muricata* seed extract and the dark brown colour of manganese oxide nanoparticles. Colour change was observed upon addition of 10 ml aqueous extract of *Annona muricata* seed to the 10 mM of permanganate solution; this indicates the formation and presence of the MnONPs in the solution.

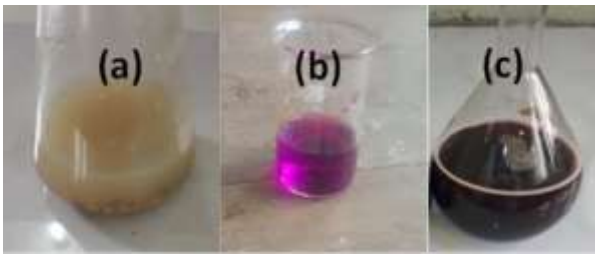

Fig. 2: *Annona muricata* seed extract (a); potassium permanganate solution (b) and manganese oxide nanoparticle solution (c)

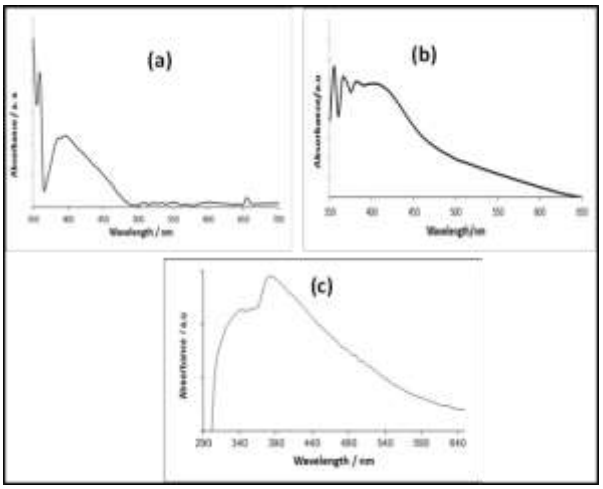

Fig. 3: UV-visible absorption spectrum of potassium permanganate (a) *Annona muricata* seed extract (b) and MnO nanoparticles (c)

UV-visible spectroscopy analysis

UV–visible spectroscopy is a powerful technique in ascertaining the formation and stability of metal nanoparticles in aqueous solution (Solomon and Jaji, 2015). Metallic nanoparticles display characteristic optical absorption spectra in the UV–visible region called surface plasmon resonance (SPR) which is due to the physical absorption of light by metallic nanoparticles, and this leads to a coherent oscillation of the conduction electron (Fig. 3). This is a small particle effect since it is absent in individual atoms as well as in their bulk structures (Kreibig and Volmer, 1995). The position of SPR is also dependent on size and shape of the particles. The UV-Visible absorption spectrum of the extract and the synthesized MnO nanoparticles were measured on a Jenway 6405 UV-visible spectrophotometer in the range of 290 to 800 nm. Fig. 3b represents the UV–visible spectra of *Annona muricata* seed extract and Fig. 3c represents the UV–visible spectra of MnO nanoparticles synthesized using *Annona muricata* seed. The UV–visible spectra of MnO nanoparticles show the characteristic fingerprint of the surface plasmon resonance (SPR) spectra with absorbance at 310–700 nm with peak maxima at ~380 nm, which can be attributed to the formation of MnO nanoparticles The shape of the plasmon band was almost symmetrical,suggesting that the nanoparticles are well dispersed and uniform. Non-uniformity of the nanoparticles leads to a broad absorption peak at higher wavelength and the splitting of a plasmon band into two bands (Baia *et al.*, 2007).

Also, the shift to lower wavelength of the spectrum indicates that the size of the MnO nanoparticle is small since optical absorption spectrum shifts to lower wavelength with decreasing particle size. 360 and 376 nm have been reported as SPR of MnO nanoparticle (Haneefa *et al.*, 2017; Karpagavalli *et al.*, 2017). Multiple peaks observed for the *Annona muricata* seed extract may be due to the phytochemicals present in the extract.

FTIR spectroscopy analysis

FTIR measurements were done for both the aqueous fresh *Annona muricata*seed extract and the synthesized dried MnO NPs to identify the possible biomolecules responsible for the reduction of Mn^{7+} ions and capping of the reduced manganese nanoparticles synthesized using *Annona muricata* seed extract. The FTIR spectra of the seed extract and the synthesized MnO NPs are shown in Fig. 4.

The spectrum was recorded in the wavelength region between 500 and 4000 cm^{-1}, with peaks depicted at different bands. The FTIR spectra bands for the seed extract were depicted at 1035,1206, 1193, 1320, 1619, 1456, 2920 – 2851 and 3314 cm^{-1} related to: C=O bonds of ether, phenols, ester (1035), C─N stretch of aliphatic amines (1206), C─N stretch of aromatic amines (1320), C=C stretching of aromatic (1619), C─C stretch of aromatics (1456), aliphatic C-H stretching and aldehydes (2920─2851), O-H stretch, H-bonded alcohols, phenols group (3314).

For the MnO nanoparticles the bands were obtain at 1035, 1205, 1342, 1431, 1587, 3242─3364 cm^{-1}, which are related to: C=O bonds of ether, phenols, ester (1035), C─N stretch of aliphatic amines (1205), C─N stretch of aromatic amines (1342), N–O symmetric stretch of nitro compounds (1342), C–C stretch (in–ring) aromatics (1431), N–H bend 1° amines (1587), O–H stretch, H–bonded of alcohols, phenols (3266─3380).

By comparing both spectra, we can conclude that the two spectra have similar spectral features. It can be said that the compound on the surface of MnO nanoparticles has very close chemical composition to the seed. It was found that many peaks obtained by the *Annona muricata*seed extract have been repeated in the FTIR spectrum of MnO nanoparticles with changes in the position as well as the intensity of absorption.

The absorption peaks at 1320, 1619, 1456 cm^{-1} corresponding to C─N stretch of aromatic amines (1318), C=C stretching of aromatic (1619), C─C stretch of aromatics (1456) observed in the plants extract got narrower and shifted to other frequency regions, while those at around 2920─2851 cm^{-1} assigned to aliphatic C-H stretching of aldehydes seems to gradually disappear and becomes negligible also, the peak at 3314 cm^{-1} corresponding to O-H stretch, H-bonded alcohols, phenols becomes broaden and shifted to frequency range of 3389─3266 cm^{-1} for the MnO nanoparticles. This indicates that water soluble compound such as phenols; alcohols and terpenoids are present in the seed extract. Hence, it can be deduced that biomolecules containing aldehyde and phenolic groups present in *Annona muricata*seed extract might be responsible for the reduction of Mn^{7+} to MnO NPs and stabilizing it.

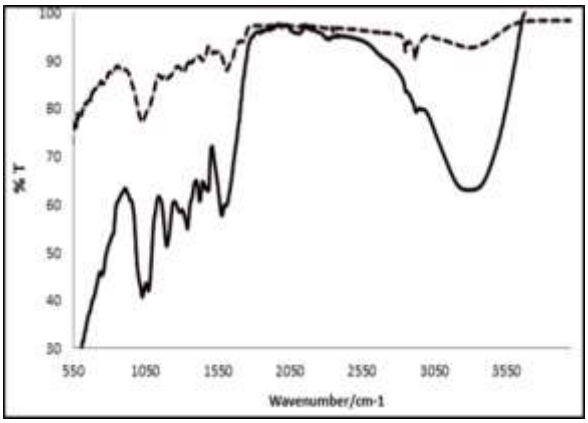

Fig. 4: FTIR spectra of *Annona muricata* seed extract (dashed line) and MnO nanoparticles (solid line)

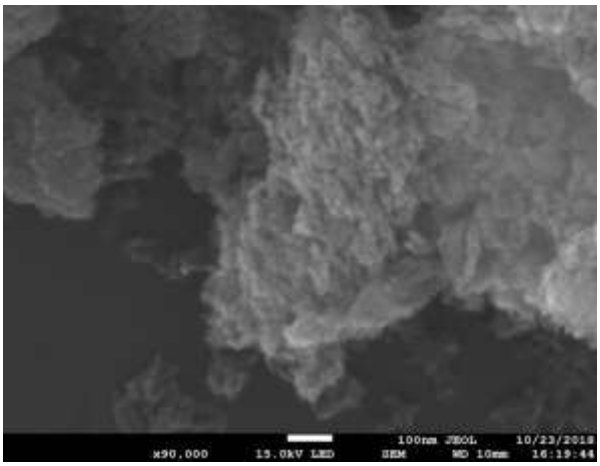

Fig. 5: SEM micrograph of manganese oxide Nanoparticles

Scanning electron microscopy (SEM) analysis

SEM micrographs were taken at 95000x magnification to study the surface morphology of the prepared manganese oxide nanoparticles. As shown in Fig. 5, most particles of the manganese oxide nanoparticles sample were spherical in shape. These spherical particles appeared smooth and uniform in size which exhibits the agglomeration that occurred during the synthesis process. It can be viewed that the MnONPs formed are moderately dispersed and slightly agglomerated. The SEM image having spherical geometry consists of a variety of pores probably due to the evolution of gases that are formed as by product during synthesis (Pradeep *et al.*, 2014).

X-ray diffraction analysis

Figure 6 shows the XRD pattern of MnO nanoparticles as tetragonal primitive centred MnO (JCPDS #24-0735) with peaks at 37.328 (101), 42.823 (111), 56.652 (211), 64.828 (002), (the numbers in bracket represents the lattice planes).

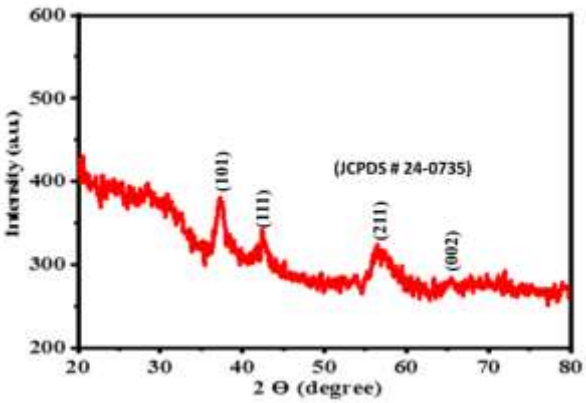

Fig. 6: X-ray diffraction pattern of manganese oxide nanoparticle

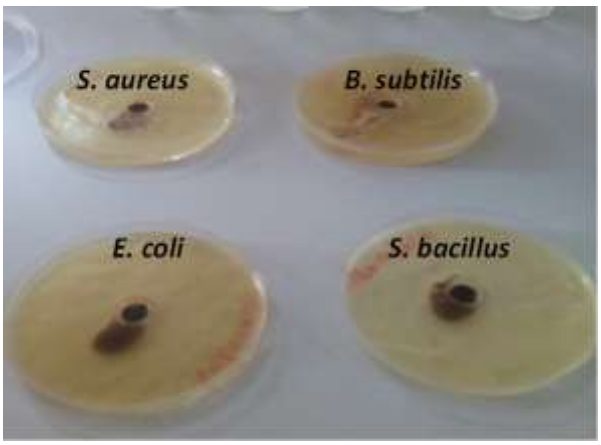

Fig. 7: Antibacterial activity showing zones of inhibition

Anti-bacterial analysis

The results of the quantitative antibacterial assessment by disc diffusion are shown in Table 1 and it was observed that the inhibition zone of *Annona muricata* seed extract synthesized manganese oxide nanoparticles was lower than the standard drug, chloramphenicol for all bacterial strains except for *S. aureus*. The MnO NPs exhibited the strongest antibacterial activity against *S. aureus* and *E. coli* and it showed moderate activity against *S. bacillus.*

Table 1: Effect of manganese oxide nanoparticles on antibacterial activity

Bacterial species (Chloramphenicol)	Zone of inhibition diameter (mm /sample)	
	Standard drug nanoparticles	Manganese oxide
S. *aureus*	16	17
B. subtilis	18	12
E. coli	20	18
S. bacillus	21	16

Therefore the presence of an inhibition zone clearly indicates that the antibacterial activity of synthesized manganese nanoparticles against *S. aureus* is superior to the standard drug, chloramphenicol and nearly similar activity against *E. coli* bacteria. The mechanism of bactericidal effect of

manganese oxide nanoparticles against bacteria is not well-known; however, manganese oxidenanoparticles may attach to the cell membrane surface and interrupt permeability and respiration associated power functions. The particles bind to the bacteria for interaction based on the available surface area. Nanoparticles having small size with larger surface area will provide better bactericidal effect as compared to the larger particles. This suggests the possibility of manganese oxide nanoparticles penetrating inside the cells of bacteria where these may cause damages by interacting with sulphur and phosphorus-containing compounds such as DNA. The other possibility may involve release of manganese ions from nanoparticles which may contribute additionally towards antimicrobial properties of manganese oxide nanoparticles. Currently, the increasingbacterial resistance against antimicrobial agents is considered as the most serious problem to treat infectious diseases. Increasingly, newer bacterial strains (both Gram-positive and Gram-negative) have been reported with an alarming high level of resistance. Precautions for preventing the emergence and spread of multi resistant bacterial strains along with the development of new antimicrobial substances are highly necessitated to deal with bacterial resistance therefore the antibacterial activity showed by manganese oxide nanoparticlesmay serve as a promising candidate for the treatment of infectious diseases since result from the test was significantly high for *S. aureus.*

Conclusion

Manganese oxide nanoparticles were successfully synthesized using *Annona muricata*seed extract. UV-visible spectrum analysis gave an SPR at ~380 nm indicating the formation of manganese oxide nanoparticles, SEM micrograph showed a spongy-like agglomeration of smooth particles. The antimicrobial evaluation of the nanoparticlesshowed better inhibition activity than the standard drug against *S. aureus*, and also exhibited similar inhibition activity to standard drug against *E. coli*. Thus our findings report MnO nanoparticles synthesized from the above proposed green method as a promising candidate in the view of pharmaceutical and therapeutic applications.

Acknowledgement

The authors will like to thank the University of Jos for providing facilities used in carrying out this work.

Conflict of Interest

Authors have declared that there is no conflict of interest reported in this work.

References

Azam A, Ahmed AS, Oves M, Khan MS, Habib SS & Memic A2012. Antimicrobial activity of metal oxide nanoparticles against gram-positive and gram-negative bacteria: A comparative study. *Intern J. Nanomed*, 7: 6003–6009.

Baia L, Muresan D, Baia M, Popp J & Simon S 2007. Structural properties of silver nanoclusters-phosphate glass composites. *Vib. Spectrosc*, 43: 313–318.

ChavaliMS &Nikolova MP 2019. Metal oxide nanoparticles and their applications in nanotechnology. *SN. Appl. Sci.*, 1: 607 https://doi.org/10.1007/s42452-019-0592-3

Chen H & He J2008. Facile synthesis of monodisperse manganese oxide nanostructures and their application in water treatment. *J. Phys. Chem. C*, 112: 17540-17545.

Gomes BP, Ferraz CC, Vianna ME, Rosalen PI, Zaia AA & Teixeira FB 2002. In vitroantimicrobial activity of calcium hydroxide pastes and their vehicles against selected microorganisms. *Braz. Dent. J.* 13(3): 155-161.

Haneefa M, Jayandran M & Balasubramanian V 2017. Evaluation of antimicrobial activity of green-synthesized manganese oxide nanoparticles and comparative studies with curcuminaniline functionalized nanoform. *Asian J. Pharm. Clin. Res.*, 10(3): 347-352.

Jayandran M, Haneefa MM & Balasubramanian V 2015. Green synthesis and characterization of manganese nanoparticles using natural plant extracts and its evaluation of antimicrobial activity. *J. Appl. Pharm. Sci.*, 5(12): 105-110.

Karpagavalli S, Vethanathan SJK, Perumal S, Koilpillai DP & Suganthi A 2017. A comparative study of optical and magnetic properties of undoped and cobalt doped manganese oxide nanoparticles *IOSR J. Appl. Phys. National Conf. on Current Advancements in Phy.*, pp. 34-42.

Kreibig U & Vollmer M 1995. Optical Properties of Metal Clusters Springer Berlin.

Krishnan B & Mahalingam S 2017. Facile synthesis and antimicrobial activity of manganese oxide/bentonitenano composites. *Res. Chem. Intermed.*, 43: 2351–2365.

Mamuru SA & Jaji N 2015. Voltammetric and impedimetric behaviour of phytosynthesized nickel Nanoparticles. *J. Nanostruct Chem.* 5: 347–356.

Ng LY, Mohammad AW, Leo CP & Hilal N 2018. Polymeric membranes incorporated with metal/metal oxide nanoparticles: A comprehensive review. *Desalination*, 308: 15-33.

Ogunyemi SO, Zhang F, Abdallah Y, Zhang M, Wang Y, Sun G, Qiu W & Li B 2019. Biosynthesis and characterization of magnesium oxide and manganese dioxide nanoparticles using *Matricariachamomilla* L. extract and its inhibitory effect on *Acidovoraxoryzae* strain RS-2. *Artificial Cells, Nanomed, and Biotech.*, 47(1): 2230–2239.

Pradeep KBM, Sriram K, Hari KR, Udayashankara TH, Shivaprasad KH & Nagabhushana BM 2014. Synthesis, characterization of nano MnO_2 and its adsorption characteristics over an azo dye. *Research and Reviews*: *J. Mat. Sci.*, 2(1): 27-31.

Singh J, DuttaT & Kim K 2018. 'Green' synthesis of metals and their oxide nanoparticles: Applications for environmental remediation. *J. Nanobiotechnol.*, 16: 84 https://doi.org/10.1186/s12951-018-0408-4

Wang N, Cao X, He L, Zhang W, Guo L & Chen C2008. One-pot synthesis of highly crystallined λ-MnO_2 nanodisks assembled from nanoparticles: Morphology evolutions and phase transitions. *J. Phys. Chem. C*, 112: 365-369.

Xiao W, Wang D & Lou XW.2010. Shape-controlled synthesis of MnO_2 nanostructures with enhanced electrocatalytic activity for oxygen reduction. *J. Phys. Chem., C*, 114: 1694-700.